

This article was downloaded by:

On: 28 January 2011

Access details: *Access Details: Free Access*

Publisher *Taylor & Francis*

Informa Ltd Registered in England and Wales Registered Number: 1072954 Registered office: Mortimer House, 37-41 Mortimer Street, London W1T 3JH, UK



Physics and Chemistry of Liquids

Publication details, including instructions for authors and subscription information:

<http://www.informaworld.com/smpp/title~content=t713646857>

Hard and Soft-Core Equations of State for Simple Fluids. X. Characteristic Curves and Loci of C_p Extrema for the Lennard-Jones 6-12 Equation of State

John Stephenson^a

^a Theoretical Physics Institute, University of Alberta, Edmonton, Alberta, Canada

To cite this Article Stephenson, John(1981) 'Hard and Soft-Core Equations of State for Simple Fluids. X. Characteristic Curves and Loci of C_p Extrema for the Lennard-Jones 6-12 Equation of State', *Physics and Chemistry of Liquids*, 10: 3, 229 – 242

To link to this Article: DOI: 10.1080/00319108108079080

URL: <http://dx.doi.org/10.1080/00319108108079080>

PLEASE SCROLL DOWN FOR ARTICLE

Full terms and conditions of use: <http://www.informaworld.com/terms-and-conditions-of-access.pdf>

This article may be used for research, teaching and private study purposes. Any substantial or systematic reproduction, re-distribution, re-selling, loan or sub-licensing, systematic supply or distribution in any form to anyone is expressly forbidden.

The publisher does not give any warranty express or implied or make any representation that the contents will be complete or accurate or up to date. The accuracy of any instructions, formulae and drug doses should be independently verified with primary sources. The publisher shall not be liable for any loss, actions, claims, proceedings, demand or costs or damages whatsoever or howsoever caused arising directly or indirectly in connection with or arising out of the use of this material.

Hard and Soft-Core Equations of State for Simple Fluids†

X. Characteristic Curves and Loci of C_p Extrema for the Lennard–Jones 6–12 Equation of State

JOHN STEPHENSON

Theoretical Physics Institute, University of Alberta, Edmonton, Alberta, Canada T6G 2J1.

(Received April, 1980)

Characteristic curves and loci of C_p extrema are constructed for the Lennard–Jones 6–12 equation of state, using fitted and approximate equations of state, and the exact virial expansion at low densities. The shape of the C_p locus near its termination temperature is analyzed via the third and fourth “pressure” virial coefficients for hard-core and Lennard–Jones systems.

1 INTRODUCTION

In this final paper of this series¹ we investigate the characteristic curves and loci of C_p extrema along isotherms for the equation of state of a fluid with an intermolecular interaction of the Lennard–Jones 6–12 form. Below the Joule–Thomson inversion temperature T_C we employ a parameterized equation of state (modified Benedict–Webb–Rubin) fitted to available numerical data by Nicolas *et al.*,² which is reliable in the range $0 < \rho\sigma_0^3 < 1.2$, $0.5 < T^* < 6.0$. Near the temperature axis at low densities one may use the virial expansion. The first five virial coefficients are known exactly for the Lennard–Jones 6–12 potential.^{3–6} Also at high temperatures and moderate densities one may employ the approximate Hansen equation of state.⁷

The characteristic curves have the expected shapes, and are displayed in Figures 1–4. The equation of Nicolas *et al.* is satisfactory within its prescribed range of validity, and admits a certain degree of extrapolation beyond this,

† Work supported in part by the Natural Scientific and Engineering Research Council of Canada, Grant No. A6595.

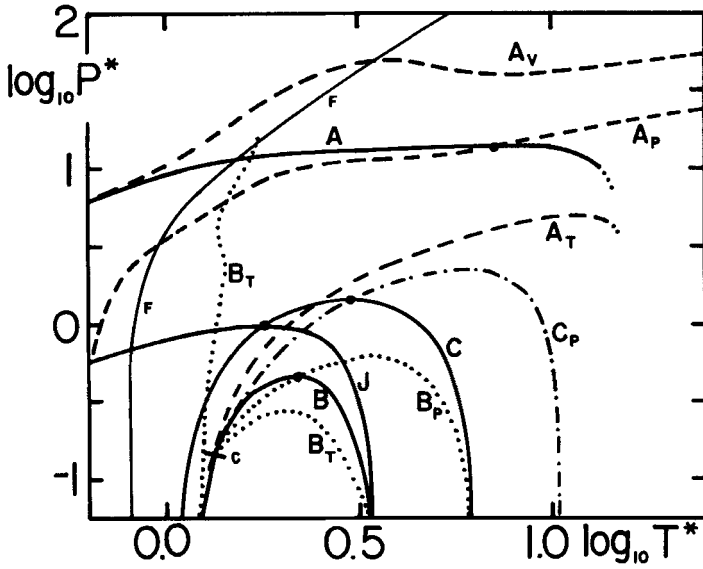


FIGURE 1 Characteristic curves for the Lennard-Jones 6-12 potential equation of state, calculated from the Nicolas *et al.* equation of state.²

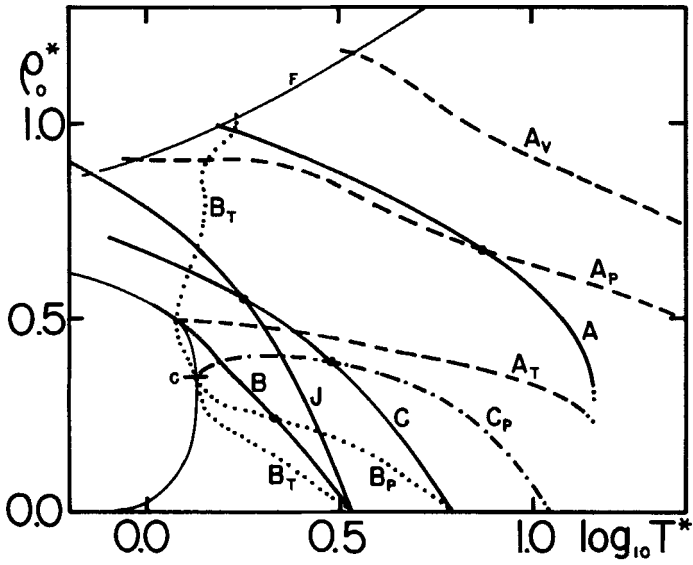


FIGURE 2 As for Figure 1.

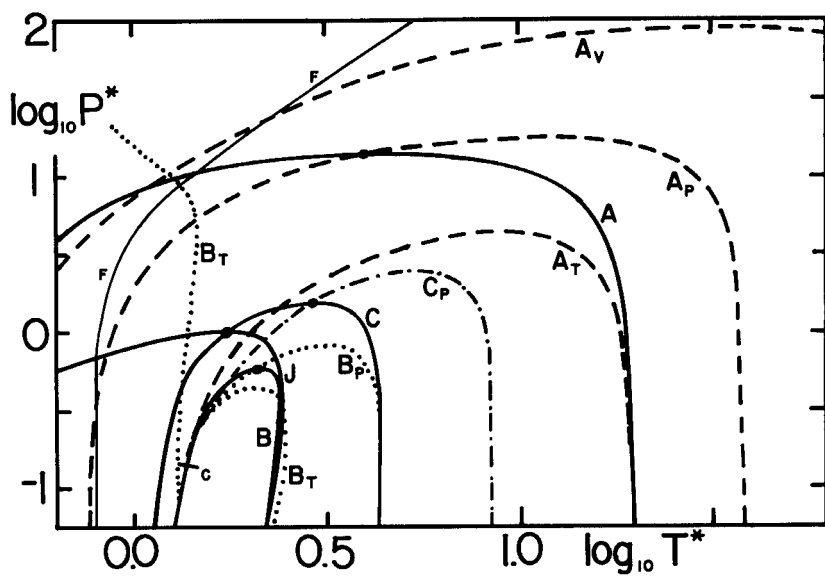


FIGURE 3 Characteristic curves for the Lennard-Jones 6-12 potential equation of state, calculated from the Hansen equation of state.⁷

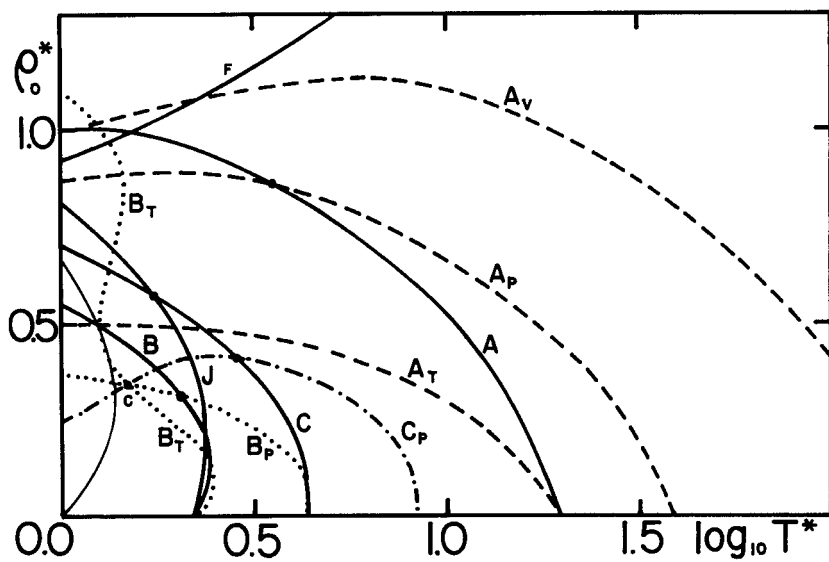


FIGURE 4 As for Figure 3.

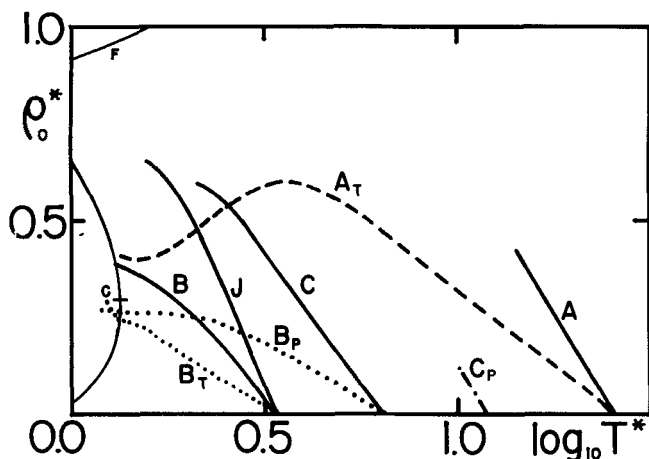


FIGURE 5 Characteristic curves for the Lennard-Jones 6-12 potential equation of state, calculated from the exact virial expansion, using up to the fourth virial coefficient D . The termination temperatures are obtained exactly from the second virial coefficient B .

although it is somewhat erroneous at low densities. This is because the six termination temperatures for the Nicolas *et al.* equation are in only rough agreement with the exact values, which may be calculated from the exact classical Lennard-Jones second virial coefficient, V . However, the virial expansion takes over at low densities and is exact, subject to satisfactory convergence of the virial series (Figure 5). Technical details are presented in Section 2.

Loci of extrema along isobars of $\rho^{m-1}(\partial T/\partial \rho)_P$ with $m = 1, 2, 3$, are presented in Figures 6 and 7. The $m = 3$ locus corresponds to extrema of C_p along isotherms (I, IX). For both the Hansen and the Nicolas *et al.* equations of state at high temperatures, we find in the vicinity of the termination temperature T_D , that a locus of C_p minima proceeds directly towards the high temperature region. Analysis of model soft-core equations of state in IX revealed this sort of behaviour to be typical of a hard-core system. At T_D the second virial coefficient has a point of inflexion. The sign of the slope of the C_p locus at T_D is determined by the curvature of the third "pressure" virial coefficient (IX):

$$C' = \frac{(C - B^2)}{RT}. \quad (1)$$

The slope is positive or negative according as $\ddot{C}' < 0$ or $\ddot{C}' > 0$, (IX(7)). ($\dot{\cdot}$ denotes temperature differentiation). For the soft-core models in IX the change in sign of the slope at T_D is associated with a "critical" value of

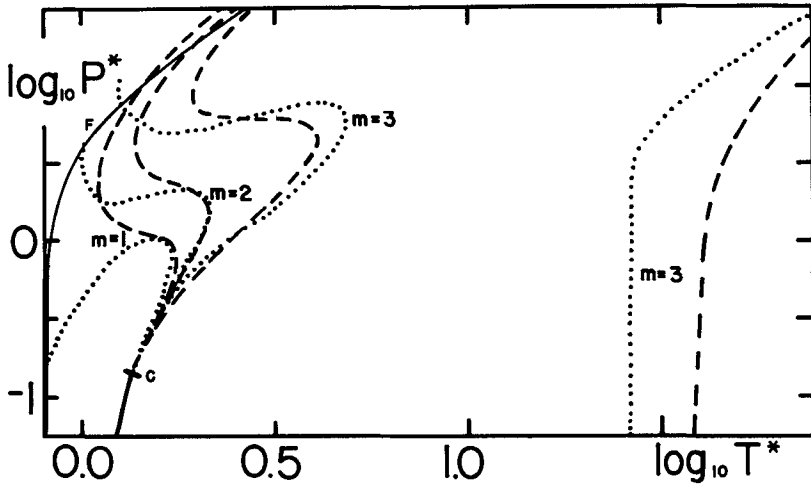


FIGURE 6 Loci of extrema of $\rho^{m-1}(\partial T/\partial \rho)_P$, $m = 1, 2, 3$, along isobars for the approximate 6–12 potential equations of state. For $m = 3$ these are loci of extrema of the constant pressure specific heat C_p along isotherms: [Loci calculated from the Nicolas *et al.* equation are “dotted,” and those from the Hansen equation are “dashed.”]

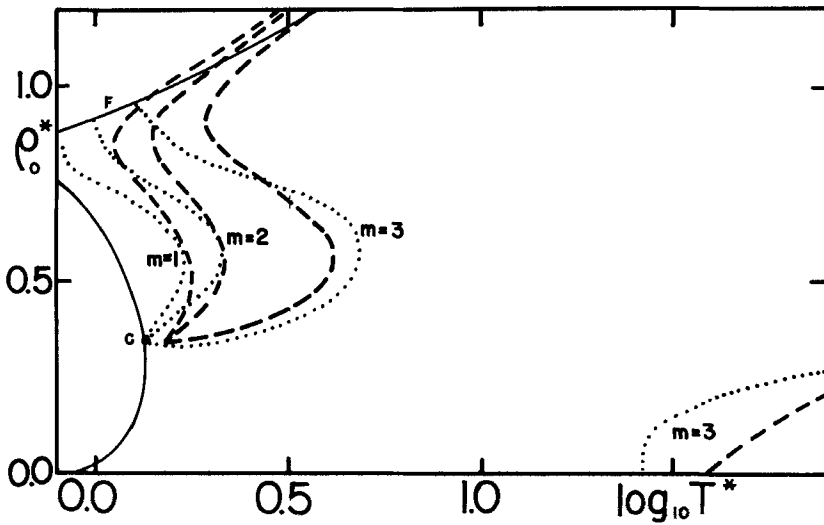


FIGURE 7 As for Figure 6.

the exponent n in the repulsive part of the intermolecular potential. For the various models (in IX) this critical value of n is 19.060946 (IX, Section 3). However, a calculation using the third "pressure" virial coefficient for the Lennard-Jones 6- n potential⁸ indicates that the corresponding critical value of the repulsive potential exponent for the Lennard-Jones model is $n_c \approx 12.2$, which is rather close to the value $n = 12$. Moreover, since $12 < n_c \approx 12.2$, the 6-12 equation of state loci would be expected to exhibit soft-core behaviour, with the C_p locus at T_D being a locus of maxima with negative slope. Since the exponent value 12 is only slightly less than the critical value 12.2, there is room for error, especially when approximate equations of state are used. This matter is investigated via the virial expansion in Section 3, where it is shown that the precise shape of the locus near T_D depends on the second temperature derivative of the fourth "pressure" virial coefficient:

$$D' = \frac{(D - 3BC + 2B^3)}{(RT)^2}. \quad (2)$$

Here B , C and D are the usual second, third and fourth "density" virial coefficients. To assist the analysis we have also looked at the corresponding virial coefficients for the hard-sphere fluid.

We conclude in Section 4 with some remarks regarding the possible significance of the theory and results presented in this series of papers, and make some suggestions for future theoretical and experimental work.

2 CHARACTERISTIC CURVES, AND TECHNICAL DETAILS OF EQUATIONS OF STATE

From the defining equations for the ten characteristic curves (II, Table I), one observes that they may be constructed numerically from an equation of state by calculating the required partial derivatives of the pressure with respect to density and temperature. The six termination temperatures come

TABLE I
Exact and approximate values of termination temperatures for the Lennard-Jones 6-12 potential second virial coefficient

Temperature	Exact, T^*	Nicolas <i>et al.</i> ²	Hansen ⁷
T_B	3.417928	3.474	2.189
T_C	6.430798	6.276	4.290
T_F	12.15737	11.325	8.409
T_A	25.15257	14.485	19.701
T_D	48.28984	26.038	38.614
T_e	203.1800	—	177.31

from the second virial coefficient, and the final slopes of the loci involve the third virial coefficient too (II, (20)–(22)). The resulting curves are displayed in Figures 1–5.

Analysis of the 33 parameter equation of Nicolas *et al.*, and the simpler equation of Hansen,⁷ is tedious but straightforward. For a Lennard–Jones 6–12 potential

$$u(r) = 4\epsilon \left[\left(\frac{\sigma_0}{r} \right)^{-12} - \left(\frac{\sigma_0}{r} \right)^{-6} \right], \quad (3a)$$

or

$$u^*(r^*) = 4[r^{*-12} - r^{*-6}], \quad (3b)$$

where u^* is scaled by the well depth ϵ , and r^* is scaled by the value of the radius σ_0 at which the potential vanishes. The position of the well bottom is at $\sigma = 2^{1/6}\sigma_0$. The scaled versions of the pressure P , number density ρ , and temperature T are then

$$P^* = P \frac{\sigma_0^3}{\epsilon}, \quad \rho^* = \rho \sigma_0^3, \quad T^* = \frac{kT}{\epsilon}, \quad (4)$$

so ρ_0^* equals the number of molecules in a volume σ_0^3 . The molecular volume parameter is defined by

$$b_0 = \frac{2\pi}{3} \sigma_0^3, \quad (5)$$

and the virial coefficients are scaled to

$$B_n^* = \frac{B_n}{b_0^{n-1}}, \quad n = 2, 3, \dots \quad (6)$$

The virial expansion then reads

$$\frac{PV}{nRT} = 1 + \sum_{n=2}^{\infty} B_n \rho^{n-1}, \quad (7a)$$

or

$$\frac{P^*}{\rho_0^* T^*} = 1 + \sum_{n=2}^{\infty} B_n^* \left(\frac{2\pi \rho_0^*}{3} \right)^{n-1}, \quad (7b)$$

where the left-hand sides of (7a) and (7b) are equal, and n' is the number of moles.

The termination temperatures are calculated from the second virial coefficient. Table I provides a comparison between the exact values and the approximate values given by the Hansen and Nicolas *et al.* second virial

coefficients, extracted from the equations of state. The agreement is rather poor. For Nicolas *et al.*,

$$B_2^* = \left(\frac{3}{2\pi}\right)(x_1 + x_2 T^{*-1/2} + x_3 T^{*-1} + x_4 T^{*-2} + x_5 T^{*-3}) \quad (8)$$

where x_1 to x_5 are in Ref. (2). And for the Hansen equation

$$B_2^* = B_1 T^{*-1/4} - C_1 T^{*-3/4}, \quad (9)$$

where

$$B_1 = \frac{2\pi}{3} 2^{1/2} \Gamma\left(\frac{3}{4}\right) = 3.629588537, \quad (10a)$$

and

$$C_1 = 5.3692. \quad (10b)$$

The full Hansen equation is quite simple in structure, and is discussed in detail in Ref. (7). The second virial coefficient (9) has some unfortunate properties at low temperatures, as noted earlier in VI. [Note that the scaled density ρ_0^* , and the density variables of Hansen⁷ and of Hoover *et al.*⁹ are all equal: to the number of molecules in a volume σ_0^3 .]

In our graphs we have used the scaled variables (4), rather than rescale relative to the critical point. The critical parameters have been estimated by Barker and Henderson¹⁰ and by Verlet and Hansen,¹¹ and lie close to the values

$$P_c^* = 0.142, \rho_{0c}^* = 0.35, T_c^* = 1.35, \quad (11)$$

quoted by Nicolas *et al.*²

The coexistence curve of Barker and Henderson¹⁰ has been used in Figures 2, 4 and 5, and the melting line (fusion curve) of Hansen and Verlet¹¹ in Figures 1–5.

The virial expansion is useful at low densities, where it takes the form

$$\frac{PV}{nRT} = 1 + B^* \rho^* + C^* \rho^{*2} + D^* \rho^{*3} + E^* \rho^{*4} + \dots \quad (12)$$

Values of the scaled second, third, fourth and fifth virial coefficients, B^* , C^* , D^* and E^* have been tabulated by Barker, Leonard and Pompe,⁵ and additional values by Henderson and Oden.⁶ It is easy to calculate B^* directly from the classical integral formula (V, where $b = 2\pi\sigma^3/3$ was used to scale B , rather than b_0 as in (6) above). Note that the virial coefficients in (12) agree with those in (6), but

$$\rho^* = \frac{2\pi}{3} \rho_0^*. \quad (13)$$

Temperature derivatives of B and C can be calculated essentially exactly,³ and elementary numerical differencing gives approximate value of \dot{D} (\dot{E} is unreliable).

When the virial expansion is employed, the more elementary characteristic curves J , A , B and C are determined by quite simple relations:

$$J: B^* + C^*\rho^* + D^*\rho^{*2} + \dots = 0, \quad (14a)$$

$$A: \dot{B}^* + \dot{C}^*\rho^* + \dot{D}^*\rho^{*2} + \dots = 0, \quad (14b)$$

$$B: B^* + 2C^*\rho^* + 3D^*\rho^{*2} + \dots = 0, \quad (14c)$$

$$C: (B^* - T^*\dot{B}^*) + (2C^* - T^*\dot{C}^*)\rho^* + (3D^* - T^*\dot{D}^*)\rho^{*2} + \dots = 0. \quad (14d)$$

There is some simplification for the higher order characteristic curves such as

$$B_T: B^* + 4C^*\rho^* + (B^*C^* + 9D^*)\rho^{*2} + \dots = 0,$$

but generally it is easier to work with the truncated virial expansions of the pressure and its partial derivatives directly. If one retains just two virial coefficients B^* and C^* , the final slopes at the termination temperatures are given correctly. One can obtain moderately satisfactory extensions of the characteristic curves into the density versus temperature phase diagram, almost up to critical density, by retaining D^* and \dot{D}^* . Including E^* does not seem to improve matters significantly. The resulting curves are displayed in Figure 5. The exact termination temperatures are calculated in V (Table I).

3 LOCI OF C_p EXTREMA ALONG ISOTHERMS

Loci of extrema of the constant pressure specific heat C_p along isotherms, and related loci of extrema of $\rho^{m-1}(\partial T/\partial \rho)_p$, $m = 1, 2, 3$, have been discussed in earlier papers of this series: for hard-core equations of state in I, fluid argon in II, and model soft-core equations of state in IX. The relevant defining formula can be written in terms of partial derivatives of the pressure with respect to density and temperature, (I(25)). Then for a given equation of state it is easy to extract the relevant loci numerically. Results for the Lennard-Jones 6-12 equation of state are presented in Figures 6 and 7.

As pointed out in the introduction, Section 1, the loci of C_p extrema appear to have a form typical of a hard-core equation of state, especially in the vicinity of the critical point and in the dense liquid near the melting line (fusion curve). However, near the termination point at T_D the shape of the C_p locus is less well resolved. The repulsive exponent value 12 is close to,

but on the soft-core side of, the “critical” exponent 12.2, at which value the slope of the C_p locus changes over from a negative “soft-core” sign to a positive “hard-core” sign. One would therefore expect that the locus of C_p extrema should commence at T_D as a locus of maxima with negative slope, which will, at some non-zero pressure and density, “double-back” as a locus of minima towards the high temperature region. This latter part of the locus might then be quite close to the forms in Figure 6 and 7 obtained from the Nicolas *et al.* and Hansen equations of state.

Near the termination point T_D one may employ the “density” and “pressure” virial expansions (for one mole, so $n' = 1$)

$$\frac{PV}{RT} = 1 + \frac{B}{V} + \frac{C}{V^2} + \frac{D}{V^3} + \dots, \quad (16a)$$

and

$$PV = RT + B'P + C'P^2 + D'P^3 + \dots \quad (16b)$$

The “pressure” (primed) virial coefficients are algebraically related to the “density” virial coefficients, with $B' = B$, and C' and D' as in (1) and (2). The C_p locus is determined by the vanishing of the derivative

$$\left(\frac{\partial C_p}{\partial P}\right)_T \equiv -T \left(\frac{\partial^2 V}{\partial T^2}\right)_P = -T[\ddot{B}' + \dot{C}'P + \ddot{D}'P^2 + \dots]. \quad (17)$$

As discussed previously in IX, the locus terminates at T_D where $B (=B')$ has a point of inflexion, and, noting that $\ddot{B}' > 0$, proceeds into the phase diagram towards lower or higher temperatures according as \dot{C}' is positive or negative. The two possible situations are illustrated in Figure 8. If we keep the fourth “pressure” virial coefficient D' , then there are two solutions for P near T_D :

$$P \approx -\frac{\ddot{B}'}{\dot{C}'} \left[1 + \frac{\ddot{B}'\dot{D}'}{\dot{C}'^2} + \dots \right], \quad (18a)$$

and

$$P \approx -\frac{\ddot{C}'}{\ddot{B}'} \left[1 - \frac{\ddot{B}'\dot{D}'}{\dot{C}'^2} + \dots \right]. \quad (18b)$$

Note that for real roots $\ddot{B}'\dot{D}'/\dot{C}'^2 \leq \frac{1}{4}$. Clearly (18a) describes the C_p locus terminating at T_D . Now (18b) offers the possibility of a second solution for P , which will be *positive* provided \dot{C}' and \ddot{D}' have opposite signs, and will be small and close to the temperature axis when $\dot{C}' \approx 0$, near the “critical” case. Presuming $\dot{C}' > 0$ (soft-core case), the second solution might now describe the “doubling-back” of the locus towards high temperatures, as in Figure 8a. The doubling-back commences at a temperature below T_D where the quad-

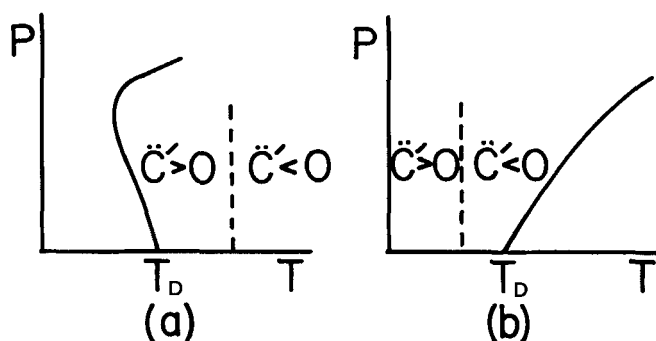


FIGURE 8 Schematic pressure versus temperature diagrams showing the possible behaviour of the locus of C_p extrema near the termination point T_D .

ratio in P in (17) has a double root and $\ddot{B}'\ddot{D}' = \frac{1}{4}\dot{C}'^2$. [The doubling-back takes place the other way round if $\dot{C}' < 0$.] Certainly this second solution will correspond to small values of P when \dot{C}' is small, but it will yield *positive* pressures only when \ddot{D}' has the opposite sign from \dot{C}' . In particular at T_D , where $\ddot{B} = 0$, the two solutions coalesce when \dot{C}' vanishes. Moreover the approach to this critical case merger takes place from the positive pressure (physical) side when \ddot{D}' and \dot{C}' have opposite signs. The description of the C_p locus near T_D and the doubling-back process therefore depend on the curvature of the fourth "pressure" virial coefficient D' .

We now investigate the temperature dependence of D' .

For the model systems in IV it appears that \ddot{D}' is *negative* near T_D . For the $T_s - N$ soft-core model, it is easy to show that the required scaled virial coefficients are

$$B^* = \frac{B}{b_0} \approx c - \frac{1}{t}, \quad (19a)$$

$$C^* = \frac{C}{b_0^2} \approx \frac{1}{16} c^2 a_2 = \frac{5}{8} c^2, \quad (19b)$$

$$D^* = \frac{D}{b_0^3} \approx \frac{1}{64} c^3 a_3 = c^3 \times 0.2869495058 \dots, \quad (19c)$$

where

$$c \equiv \frac{b}{b_0} = \frac{1}{[1 + (t/t_s)^N]}, \quad t = b_0 \frac{RT}{a}, \quad (20)$$

a and b are van der Waals type parameters, defined as in I, IV and IX, and a_2 and a_3 are hard sphere virial coefficients which are known exactly, I.

Then from (1) and (2)

$$C' = (-) \frac{b_0^3}{a} \left[\frac{3c^2}{8t} - \frac{2c}{t^2} + \frac{1}{t^3} \right], \quad (21)$$

and

$$D' = \frac{b_0^5}{a^2} \left[\frac{(a_3 + 8)c^3}{64t^2} - \frac{33c^2}{8t^3} + \frac{6c}{t^4} - \frac{2}{t^5} \right]. \quad (22)$$

The hard-core D' , with $c \equiv 1$, has been plotted versus $\log_{10} t$ in IX (Figure 9). Its features—zeros, and locations of maxima and minima and points of inflexion—are listed in Table II. Clearly D' is negative at low temperatures, positive at high temperatures, and has three zeros, two maxima, one minimum and three points of inflexion. Between the two upper points of inflexion, where $2.036 < t < 17.302$, \dot{D}' is negative. Compared with the critical temperature t_{c0} , which equals $0.375312 \dots$ for the F -model (I), the corresponding range is $5.424 < t/t_{c0} < 46.100$. This range is slightly below the range of “critical” values of t_D/t_c for the soft-core F model (IX, Table II): $44.5 < t_D/t_c < 54.96$. However, when the soft-core is inserted in (19), the range of t/t_c in which \dot{D}' is negative shifts towards higher temperatures, so as to include the termination point t_D . [For example, when $t_s = 0$, \dot{D}' is negative

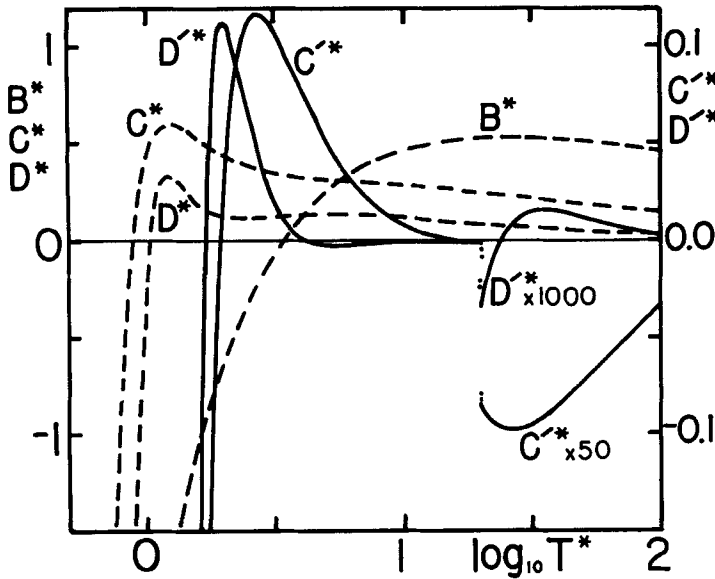


FIGURE 9 Exact second, third and fourth “density” virial coefficients, B^* , C^* , and D^* , and third and fourth “pressure” virial coefficients, C'^* and D'^* , for the Lennard-Jones 6-12 potential.

TABLE II

Features of the fourth "pressure" virial coefficient for the hard-sphere fluid, D'

Zeros	Maxima/Minima	Inflexion
0.490865	0.587911	0.689185
1.186496	1.610119	2.035774
8.336002	12.822014	17.301767

at t_D for N in the range 0.1205... to 0.8586..., which includes the "critical" case (IX).]

The situation for the Lennard-Jones 6-12 potential is rather similar. The relevant scaled virial coefficients: B^* , C^* , D^* and C'^* , D'^* may be evaluated, with the aid of the data of Barker *et al.* and Henderson and Oden, and are plotted versus $\log_{10} T^*$ in Figure 9. D^* has a high temperature minimum close to $T^* \approx 5.7$, a maximum near 35, and associated points of inflexion near 6 and between 45 and 50, so \ddot{D}^* is negative in the (approximate) range $6 < T^* < 45$ to 50. Now T_D^* for the Lennard-Jones 6-12 potential is 48.29..., towards the upper end of the range where \ddot{D}^* may be negative. If \ddot{D}^* is still negative at T_D^* , the situation for the Lennard-Jones 6-12 potential is as in Figure 8a. However, if \ddot{D}^* is positive at T_D^* , the geometry of the C_p locus would not show such a pronounced doubling back as in Figure 8a. The second solution (18b) would correspond to negative pressure. A third solution would be required at higher pressures, away from the temperature axis, to account for the subsequent progression of the locus towards the high temperature region. However, we do not consider our calculation of D^* for the Lennard-Jones 6-12 potential to be precise enough to determine unambiguously the sign of \ddot{D}^* at T_D^* .

4 CONCLUDING REMARKS

In this series of papers we have endeavoured to develop a theory of fluids in which the softening of the molecular core is taken into account. By combining exact results for virial coefficients, and hard-core equations of state, with simple models of a temperature dependent soft molecular core, we have been able to construct the overall properties of characteristic curves and loci of extrema of C_p . Especially novel has been the discovery of simple ratio relations between characteristic temperatures (IV) and the existence of "critical" values of the repulsive potential exponent (IX) which, in conjunction with a softening temperature t_s , determine the exotic shape of

the C_p locus, both in the vicinity of its termination point on the temperature axis, and in the phase diagram.

It is to be hoped that analysis of available data on virial coefficients and equations of state for simple fluid systems will reveal to what extent the variety of theoretically possible behaviours which we have discovered will be exhibited in practice. Particularly there is a need for high temperature (relative to critical) data for the second and third virial coefficients, in order to determine how our analysis of the C_p locus applies to real systems. Additional experimental data on the virial coefficients of monatomic gases which do not ionize easily would be most welcome. It would also be of interest to learn if there are any sufficiently soft-core systems that might exhibit C_p loci with a single branch from the critical point to the temperature axis, or even loci close to the saddle-point region.

On the theoretical side we plan to continue our study of Lennard-Jones m - n potential systems, via exact virial coefficients and approximate equations of state, and hence to investigate to what extent the exotic properties of the model ($T_s - N$) system are also present in this theoretically more realistic system.

A review and summary of the material developed in this series of papers is in preparation.

Acknowledgements

I would like to thank Rodney Couzens, Radha Gourishankar and H. K. Leung who have aided with the calculations in one or more papers of this series. Their contributions to both the numerical and theoretical work have been most valuable.

References

1. The previous papers in this series are: I. John Stephenson, *Phys. Chem. Liq.*, **8**, 235 (1979). II. John Stephenson and H. K. Leung, *Phys. Chem. Liq.*, **8**, 249 (1979). III. John Stephenson, *Phys. Chem. Liq.*, **8**, 265 (1979). IV. John Stephenson, *Phys. Chem. Liq.*, **9**, 23 (1979). V. John Stephenson, *Phys. Chem. Liq.*, **9**, 37 (1979). VI. John Stephenson, *Phys. Chem. Liq.*, **9**, 51 (1979). VII. John Stephenson and H. K. Leung, *Phys. Chem. Liq.*, **9**, 175 (1980). VIII. John Stephenson, *Phys. Chem. Liq.*, **10**, 153 (1980). IX. John Stephenson and Rodney Couzens, *Phys. Chem. Liq.*, **10**, 167 (1980).
2. J. J. Nicolas, K. E. Gubbins, W. B. Streett, *Molecular Physics*, **5**, 1429 (1979).
3. J. O. Hirschfelder, C. G. Curtis and R. B. Bird, *Molecular Theory of Gases and Liquids*. Preceding papers (John Wiley, New York, 1964).
4. T. Kihara, *J. Phys. Soc. (Japan)*, **3**, 265 (1948); **6**, 184 (1951).
5. J. A. Barker, P. J. Leonard and A. Pompe, *J. Chem. Phys.*, **44**, 4206 (1966).
6. D. Henderson and L. Oden, *Molecular Physics*, **10**, 405 (1966).
7. J-P. Hansen, *Phys. Rev.*, **A2**, 221 (1970).
8. J. Stephenson and H. K. Leung (to be published).
9. W. G. Hoover, M. Ross, K. W. Johnson, D. Henderson, J. A. Barker, and B. C. Brown, *J. Chem. Phys.*, **52**, 4931 (1970).
10. J. A. Barker and D. Henderson, *J. Chem. Phys.*, **47**, 4714 (1967).
11. J-P. Hansen and L. Verlet, *Phys. Rev.*, **184**, 151 (1969).